Rmi1 stimulates decatenation of double Holliday junctions during dissolution by Sgs1–Top3

Petr Cejka, Jody L. Plank, Csanad Z. Bachrati, Ian D. Hickson, and Stephen C. Kowalczykowski

Supplementary Information

Supplementary Methods

 Expression and purification of Top3. The *TOP3* gene was amplified by polymerase chain reaction (PCR) using wild type *S. cerevisiae* genomic DNA as a template (strain S288C, Research Genetics) and primer pairs PC3 (CTCTGAACTCGAGCTGGAAGTTCTGTTCCAGGGGCCC<u>GCTAGC</u>GGATCC**ATG AAAGTGCTATGTGTCGCAG**; NheI site underlined and the sequence complementary to *TOP3* in bold) and PC4 (CGCAAATC<u>CTCGAG</u>CCCGGG**TTACATGGATGCCTTGACACGG**; XhoI site underlined and the sequence complementary to *TOP3* in bold). The reaction products were digested with NheI and XhoI restriction endonucleases, and cloned into NheI and XhoI sites in modified pFastBac1 vector[1], creating pFB-GST-Top3. This placed the *TOP3* coding sequence downstream from sequence encoding glutathione-S-transferase (GST) and a PreScission protease cleavage site, all of which is under the control of the baculovirus polyhedron promoter. Proteins were expressed using the Bac-to-Bac expression system (Invitrogen) in Sf9 cells according to manufacturer's recommendations. All purification steps were carried out on ice or at 4°C.

 Top3 was harvested from 1.6 l of Sf9 cells 56 hours post-infection with the appropriate baculovirus. Sf9 cells were resuspended in 48 ml lysis buffer and proteins were extracted with salt as described previously for Sgs1[1], except 10 mM β-mercaptoethanol was used instead of 1 mM DTT in the lysis buffer. Soluble extracts were obtained by centrifugation at 58,000g for 30 min. Protein extracts were incubated batch-wise with 4 ml glutathione affinity resin (Clontech) for 1 hour. The resin was extensively washed batch-wise and then on-column with high salt wash buffer (50 mM Tris-HCl (pH 7.5), 5 mM β-mercaptoethanol, 1 M NaCl, 1 mM EDTA, 10% (v/v) glycerol, 1 mM Phenylmethanesulfonyl fluoride (PMSF), 10 μg ml^{-1} leupeptin) and then with low salt wash buffer (50 mM Tris-HCl (pH 8.0), 5 mM β-mercaptoethanol, 150 mM NaCl, 1 mM EDTA, 10% (v/v) glycerol, 1 mM PMSF, and 10 μg ml^{-1} leupeptin), and proteins were eluted with 2 column volumes of low salt wash buffer containing 10 mM glutathione.

The GST affinity tag was cleaved off the GST–Top3 fusion by incubation with PreScission protease. The NaCl concentration was then adjusted to 300 mM, and the sample was mixed with 0.5 ml preequilibrated Bio-Rex 70 resin (Bio-Rad), incubated batch wise for 15 min, and flow-through was collected by pouring the slurry into a plastic chromatography column. The sample was then diluted with dilution buffer (50 mM Tris-HCl (pH 7.5), 1 mM DTT, 1 mM EDTA, 10% (v/v) glycerol, 1 mM PMSF, and 10 µg ml^{-1} leupeptin) so that NaCl concentration was adjusted to 50 mM. Using an ÄKTA chromatography system (GE Healthcare), the sample was loaded on 1 ml HiTrap SP HP column (GE Healthcare) at 0.8 ml min^{-1}. The resin was washed with 20 ml SP buffer A (50 mM Tris-HCl pH 7.5, 1 mM DTT, 50 mM NaCl, 10% (v/v) glycerol, 1 mM PMSF, 10 µg ml^{-1} leupeptin), and recombinant Top3 was eluted with a salt gradient. Top3 eluted at ~250 mM NaCl. The sample was then aliquoted, snap frozen in liquid nitrogen, and stored at -80 °C. Protein concentration was determined by the Bradford method with bovine serum albumin as a protein standard. Typical yield from 1.6 l culture was about 1 mg, and the final protein concentration was 3–7 µM.

Expression and purification of Rmi1. The *RMI1* gene was amplified and cloned similarly to the *TOP3* gene using primer pairs PC5 (CTCTGAACTCGAGCTGGAAGTTCTGTTCCAGGGGCCC<u>GCTAGC</u>GAATTCA**TG TCTTTTTCATCTATCTTATCAC**; NheI site underlined and the sequence complementary to *RMI1* in bold) and PC6 (CGCAAATC<u>CTCGAG</u>CCCGGG**CTAATCATTGGCTTTCCTTTTC**; XhoI site underlined and the sequence complementary to *RMI1* in bold) to prepare pFB-GST-Rmi1. The *RMI1* gene was also cloned downstream from a MBP tag[1], creating pFB-MBP-Rmi1, using the same primer pair and restriction sites. Rmi1 was expressed and purified similarly to Top3, omitting the Bio-Rex 70 step. Furthermore, since the above protein preparation contained a small amount of ssDNA exonuclease contamination, we also added a His$_{(10)}$ tag to the C-terminus of Rmi1. We used primer pairs PC 36 (TAAAGCAGTGTTTAAATTGAC) and PC 65 (CGCAATCCTCGAGCTAA**ATGGTGATGGTGATGGTGATGGTGATGGTG**ATCA TTGGCTTTCCTTTTC; sequence coding for His$_{(10)}$ tag in bold) to amplify the 3' region

of the *RMI1* gene. The PCR product was digested with SacI and XhoI restriction endonucleases and cloned into SacI and XhoI sites in pFB-GST-Rmi1, creating pFB-GST-Rmi1-His. The recombinant protein was prepared by using glutathione affinity resin as described above, followed by a second affinity purification step with Ni^{2+}-nitrilotriacetic acid (NTA) agarose (Qiagen), according to the manufacturer's recommendation. The Rmi1–$His_{(10)}$ protein preparation contained no nuclease contamination and both Rmi1 and Rmi1–$His_{(10)}$ protein preparations were equally active in the assays performed in this manuscript. We typically obtained ~1 mg of Rmi1 at a concentration ~10 μM.

Expression and purification of Top3–Rmi1 heterodimer. Top3-Rmi1 heterodimer was obtained by coexpressing the GST–Top3 and MBP–Rmi1 fusion proteins. The Sf9 cells were lysed and protein extract was incubated with glutathione affinity resin as detailed above for Top3 purification. However, the resin was then washed with buffer containing only 250 mM NaCl, in order not to disrupt the Top3–Rmi1 heterodimer. Following elution with glutathione, the sample was applied on preequilibrated amylose affinity resin (New England Biolabs), incubated batch wise for 1 hour, and eluted with MBP elution buffer (50 mM Tris-HCl (pH 7.5), 10 mM β-mercaptoethanol, 150 mM NaCl, 1 mM EDTA, 10% (v/v) glycerol, 1 mM PMSF, 10 μg ml^{-1} leupeptin, and 10 mM maltose). The protein was then cleaved by PreScission protease and further purified on 1 ml HiTrap SP HP column as described above. We typically obtained ~1 mg of the heterodimer at a concentration of ~2-5 μM from 1.6 l cell culture.

Supplementary References

1   Cejka, P. & Kowalczykowski, S. C. The full-length S. cerevisiae SGS1 protein is a vigorous DNA helicase that preferentially unwinds Holliday junctions. *J. Biol. Chem.* **285**, 8290-8301, (2010).
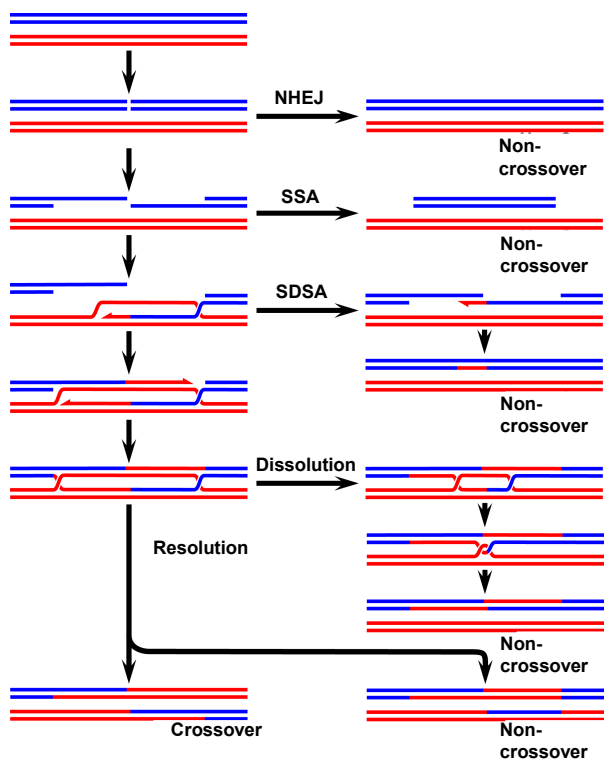
Supplementary Figure 1 Schematic representation of recombination pathways that lead to crossovers *versus* non-crossovers in homologous recombination. Double-stranded DNA breaks may be repaired by non-homologous end joining (NHEJ) or one of several homologous recombination (HR) pathways. Sgs1 has been proposed to disrupt joint molecules and promote the synthesis-dependent strand annealing (SDSA) pathway. Sgs1 contributes to extensive 5' DNA end resection by nucleases, which could promote the single-strand DNA annealing (SSA) pathway by revealing the homologies required for this pathway. Both SDSA and SSA pathways lead exclusively to non-crossover products. Finally, in the canonical HR model pathway leading to double Holliday junctions (dHJs), Sgs1, Top3, and Rmi1 promote dissolution leading to non-crossovers as opposed to the alternative resolution by nucleolytic cleavage leading to both crossover and non-crossover recombination products.
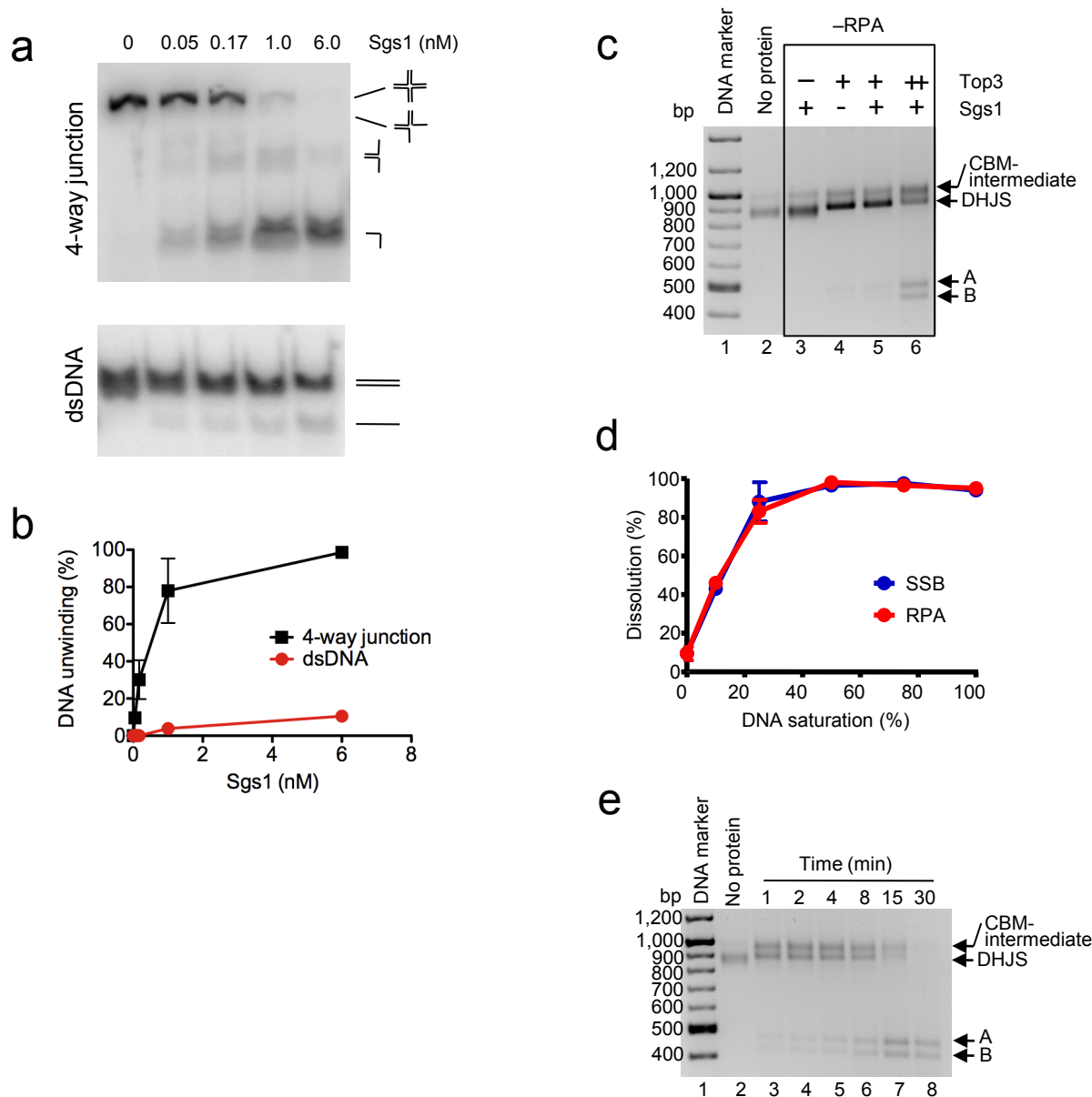
Supplementary Figure 2 Sgs1 and Top3, stimulated by replication protein A (RPA) or SSB, dissolve double Holliday junctions. (**a**) Sgs1 preferentially unwinds a 4-way junction. The indicated concentrations of Sgs1 were incubated in dissolution buffer with a labeled oligonucleotide-based 4-way junction or with dsDNA (both at 0.15 nM molecules) in the presence of unlabeled competitor pUC19 dsDNA (3.85 μM, base pairs) for 30 min. The amount of competitor dsDNA equals to the amount of dsDNA in the DHJS dissolution assays. The reaction products were separated on a 10% polyacrylamide gel. The panel shows a representative experiment. (**b**) Quantification of the data from experiments such as those shown in panel **a**. Error bars, s.e.m. (**c**) Sgs1 and Top3 can dissolve the DHJS in the absence of RPA, albeit at a lower efficiency. Sgs1 (6 nM) and/or Top3 (36 or 360 nM) were incubated with the DHJS as described in the Methods. The "CBM-intermediate" denotes the convergently branch-migrated intermediate with a reduced mobility relative to the DHJS. (**d**) Sgs1 and Top3 are stimulated equally by RPA or SSB. Quantification of the dissolution reactions carried out with Sgs1 (6 nM), Top3 (36 nM), and varying concentrations of RPA or *E. coli* SSB. The x-axis denotes the potential percentage of DNA binding by the respective ssDNA binding protein; 100% DNA saturation corresponds to 385 nM RPA and 480 nM SSB, respectively (see Methods for details). Error bars, s.e.m. (**e**) Time course of DHJS dissolution. Reactions containing Sgs1 (6 nM), Top3 (36 nM), and RPA were terminated at the indicated times. The "CBM-intermediate" denotes the convergently branch-migrated intermediate with a reduced mobility relative to the DHJS.
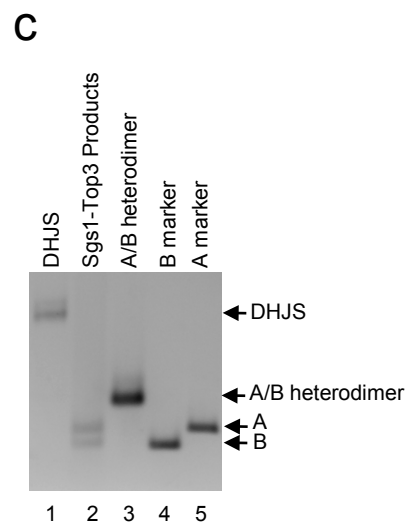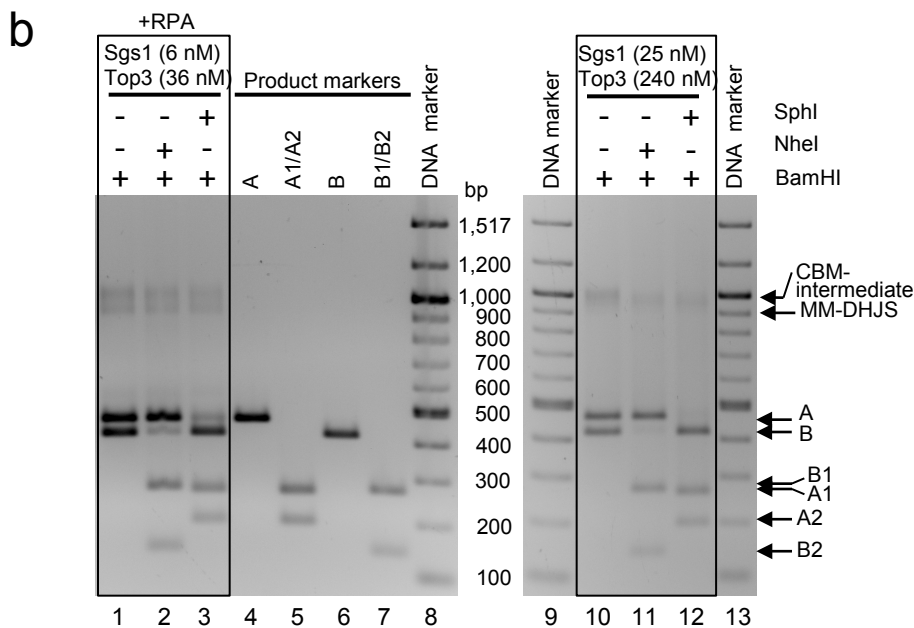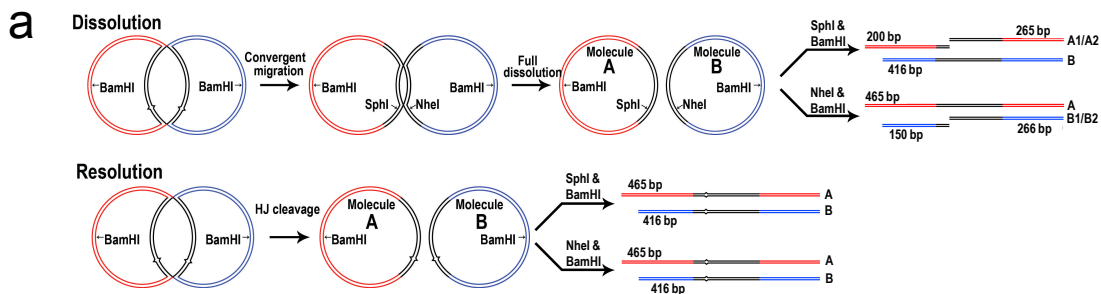
Supplementary Figure 3 Processing of dHJ by Sgs1 and Top3 occurs through convergent branch migration. (**a**) A schematic representation of a modified DHJS containing mismatches (MM-DHJS). Resolution of the MM-DHJS by nucleolytic cleavage preserves the mismatches, leaving the reaction products insensitive to cleavage by NheI and SphI. Dissolution through convergent branch migration creates the restriction sites and yields products susceptible to NheI and SphI cleavage: the positions of the BamHI, SphI and NheI sites are indicated. (**b**) MM-DHJS was incubated with the indicated concentrations of Sgs1, Top3, and RPA (578 nM, when present). Reaction products were purified, digested by the indicated restriction endonucleases, and analyzed by electrophoresis. Lanes 4-7 contain the product size markers: Markers A and B were generated as described in the Methods and digested with BamHI (A and B) or BamHI and NheI (A1/A2 and B1/B2). The "CBM-intermediate" denotes the convergently branch-migrated intermediate with a reduced mobility relative to the DHJS. The reaction products are sensitive to NheI or SphI cleavage, which indicates convergent branch migration of the HJs. (**c**) HJs migrate through homologous, and not heterologous region between the junctions. The products of a dissolution reaction containing Sgs1 (36 nM), Top3 (77 nM), and RPA (lane 2) comigrate with A and B molecules (lanes 4 and 5), the expected products of branch migration through the homologous region. Migration in the opposite direction (i.e., through heterology) would restore A/B and B/A heterodimers, the intermediates in DHJS preparation (lane 3). All DNA molecules were digested with BamHI prior to electrophoretic analysis.
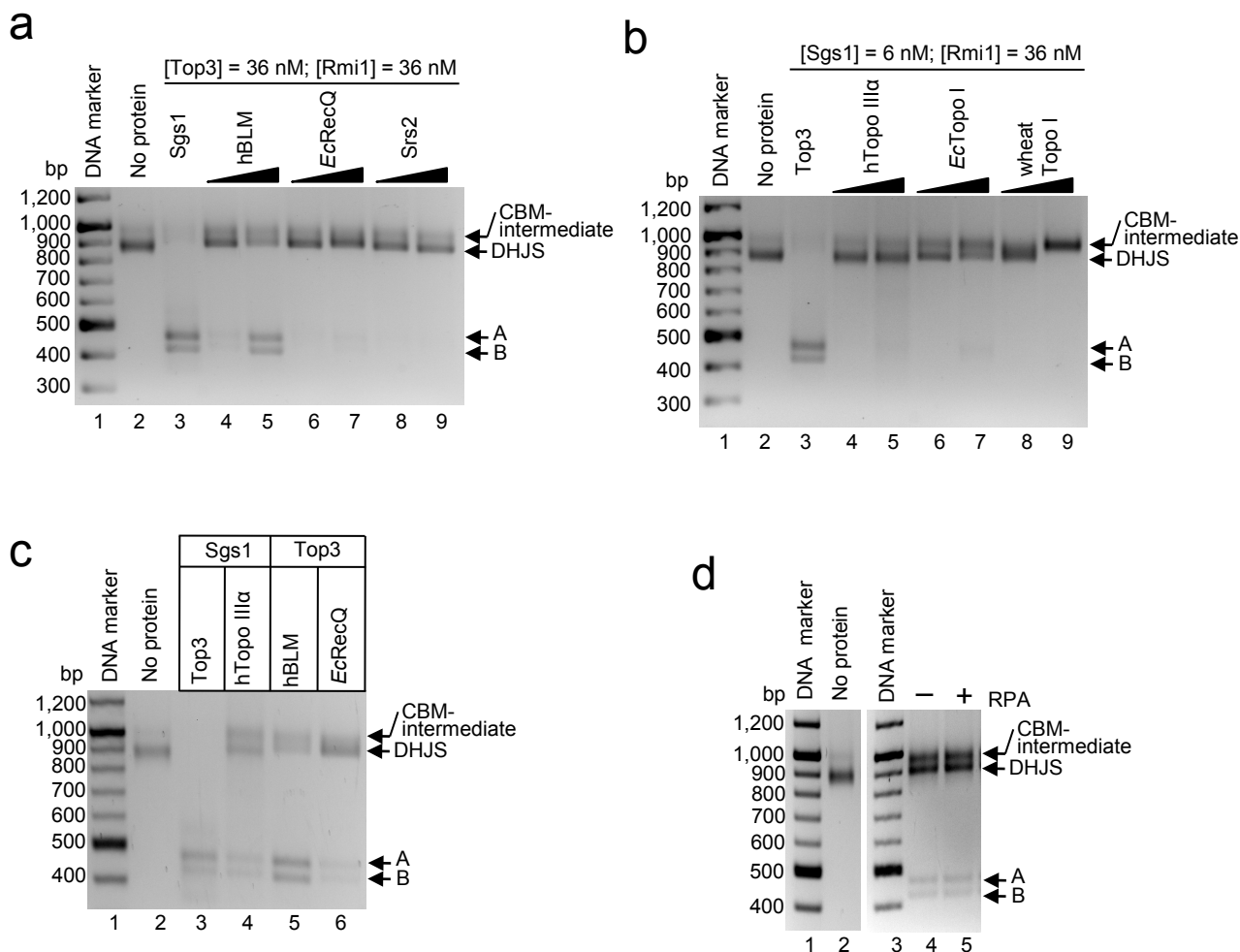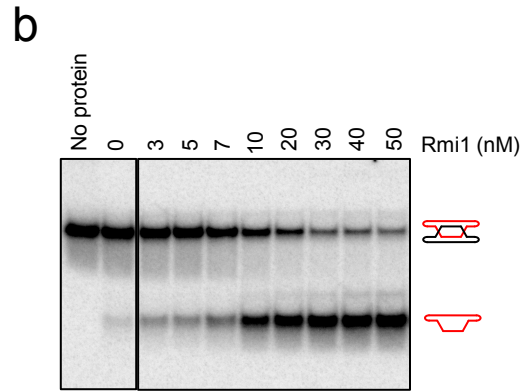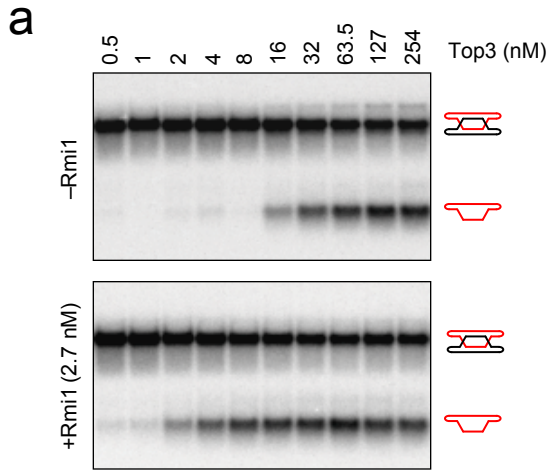
Supplementary Figure 4 The dissolution of dHJs is optimal with the cognate Sgs1 and Top3 protein pair. (**a**) Inclusion of yeast Rmi1 does not improve the efficiency of dissolution reactions performed with non-cognate helicases. Dissolution reactions were carried out with RPA (578 nM), Top3 (36 nM), Rmi1 (36 nM) and either yeast Sgs1 (6 nM, lane 3), human BLM (6 and 36 nM, lanes 4 and 5, respectively), *E. coli* RecQ (6 and 36 nM, lanes 6 and 7, respectively), or another *S. cerevisiae* helicase with 3'-5' unwinding polarity, Srs2 (6 and 36 nM, lanes 8 and 9, respectively). (**b**) Inclusion of yeast Rmi1 does not improve the efficiency of dissolution reactions performed with non-cognate topoisomerases. Dissolution reactions were carried out with RPA (578 nM), Sgs1 (6 nM), Rmi1 (36 nM) and either yeast Top3 (36 nM, lane 3), human Topo IIIα (36 and 100 nM, lanes 4 and 5, respectively), *E. coli* Topo I (2.5 and 10 units, lanes 6 and 7, respectively), or wheat germ Topo I (2.5 and 10 units, lanes 8 and 9, respectively). (**c**) Dissolution can occur at high concentrations of non-cognate helicases and topoisomerases. The reactions contained, as indicated, Sgs1 (36 nM), human BLM (36 nM), *E. coli* RecQ (36 nM), Top3 (150 nM), human Topo IIIα (150 nM), and RPA (578 nM). (**d**) High concentrations of Top3 show a limited capacity to dissolve dHJ in the absence of a helicase. The DHJS dissolution reaction contained Top3 (360 nM) and RPA (578 nM), where indicated. Dissolution likely occurs through spontaneous thermal branch migration, and simultaneous strand passage catalyzed by Top3, due to a "random walk" by one or both HJs. "CBM-intermediate" in all panels indicates the position of the DHJS with convergent branch migration of the HJs.
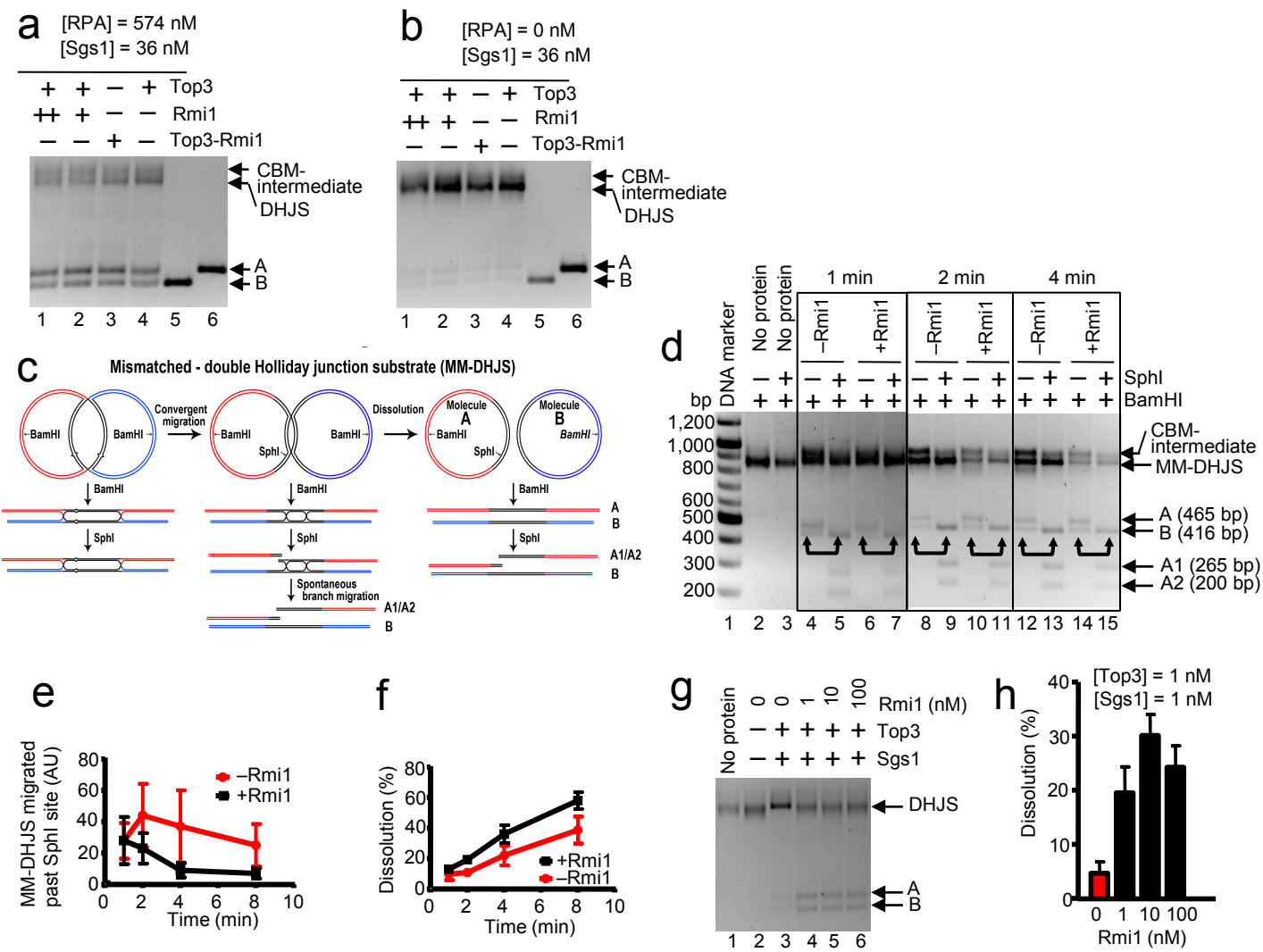
Supplementary Figure 5 Rmi1 stimulates dissolution of dHJs at low concentrations of Sgs1 and Top3. (**a**) Dissolution of the DHJS by high concentrations of Sgs1 and Top3, in the presence of RPA, is not stimulated by Rmi1. The reactions contained Sgs1 (36 nM), Top3 (36 nM), Top3-Rmi1 heterodimer (36 nM), and Rmi1 (360 nM, lane 1; 36 nM, lane 2, respectively), as indicated, and RPA (578 nM). A and B markers represent the expected reaction products (lanes 5, 6). (**b**) In the absence of RPA, dissolution of the DHJS by high concentrations of Sgs1 and Top3, is not stimulated by Rmi1. The reactions contained Sgs1 (36 nM), Top3 (36 nM), Top3-Rmi1 heterodimer (36 nM) and Rmi1 (360 nM, lane 1; 36 nM, lane 2, respectively), as indicated. A and B markers represent the expected reaction products (lanes 5, 6). "CBM-intermediate" indicates the position of the DHJS with convergent branch migration of the HJs. (**c**) The MM-DHJS was used to detect the formation of the branch migration intermediate by restriction analysis. See Figure 2 and text for more details. (**d**) Rmi1 moderately promotes dissolution of dHJs catalyzed by intermediate concentrations of Sgs1-Top3. Restriction analysis of the time course dissolution of MM-DHJS. The reactions were carried out with Sgs1 (6 nM), either Top3 (36 nM, denoted as "-Rmi1") or Top3-Rmi1 heterodimer (36 nM, denoted as "+Rmi1"), and RPA (578 nM), and terminated at the indicated times. The amount of the intermediate formed by partial HJ migration past the mismatch site corresponds to the amount of the 416 bp band generated by digestion with BamHI and SphI minus the amount of the 416 bp band generated from BamHI digestion alone, as indicated. Early (at 1 minute), the amount of the intermediate is similar without and with Rmi1, as detected by the similar intensity differences of the indicated bands in lanes 4 vs. 5, and 6 vs. 7. Later (at 4 min), there is more branch-migrated intermediate in reactions without Rmi1 (compare the relatively high intensity difference of the indicated bands in lanes 12 vs. 13 to the low intensity difference of the indicated bands in lanes 14 vs. 15). At the 2 and 4 minute time points, the reactions which contain Rmi1 (lanes 10, 11, 14, and 15) appear to contain less substrate than the Rmi1 controls. This is due to the catenation activity of Sgs1-Top3-Rmi1 at these concentrations, which retards the electrophoretic mobility of some of the unresolved DHJS. This activity does not affect the linear molecules generated by restriction digestion and, therefore, does not affect the quantification of the experiment. (**e**) Quantification of experiments such as those shown in panel **d** showing the amount of the intermediate migrated past the SphI site (see panel **c**) during the course of MM-DHJS dissolution. The Y-axis shows arbitrary sums of pixel intensity values. Error bars, s.e.m. (**f**) Kinetics of MM-DHJS dissolution, based on experiments such as those shown in panel **d**. (**g**) Rmi1 stimulates DHJS dissolution at low Sgs1 and Top3 concentrations. DHJS was incubated with Sgs1 (1 nM), Top3 (1 nM), and the indicated concentration of Rmi1, in the presence of RPA (578 nM). (**h**) Quantification of experiments such as those shown in panel **g**. Error bars, s.e.m.

Supplementary Figure 6 Rmi1 stimulates the dissolution of oligonucleotide-based dHJ DNA. (**a**) Dissolution of the oligonucleotide-based dHJ DNA is stimulated by Rmi1 at low Top3 concentrations. Reactions contained Sgs1 (0.22 nM), Top3 as indicated, and Rmi1 (2.7 nM) where indicated. (**b**) The Rmi1 concentration dependence of dissolution by Sgs1 and Top3. Reactions contained Sgs1 (0.56 nM), Top3 (3.2 nM), and the indicated concentrations of Rmi1.
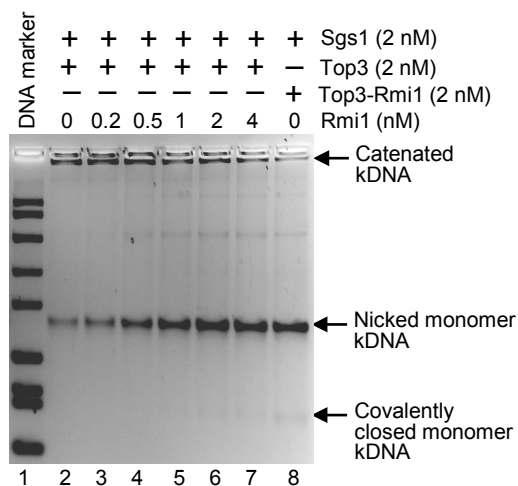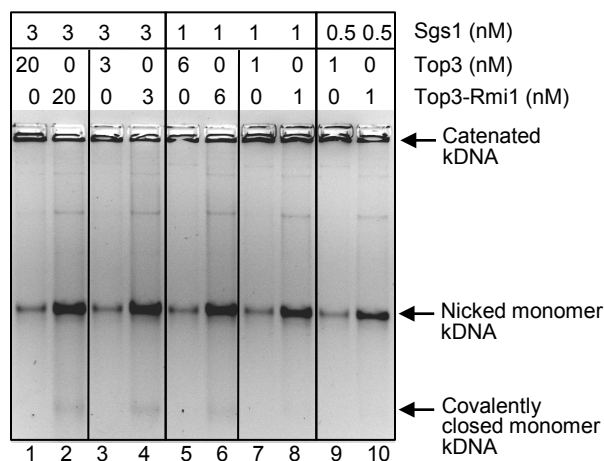
Supplementary Figure 7 Rmi1 greatly promotes decatenation of kinetoplast DNA (kDNA). (**a**) Decatenation of kDNA is dependent on Rmi1 concentration. The reactions contained RPA (340 nM), Sgs1 (2 nM), Top3 (2 nM, lanes 2-7) or Top3-Rmi1 heterodimer (2 nM, lane 8), and varying concentrations of Rmi1, as indicated. (**b**) The stimulation of kDNA decatenation by Rmi1 occurs over range of protein concentrations. The reactions contained RPA (340 nM), Sgs1, and either Top3 or Top3-Rmi1 heterodimer, at the concentrations indicated.
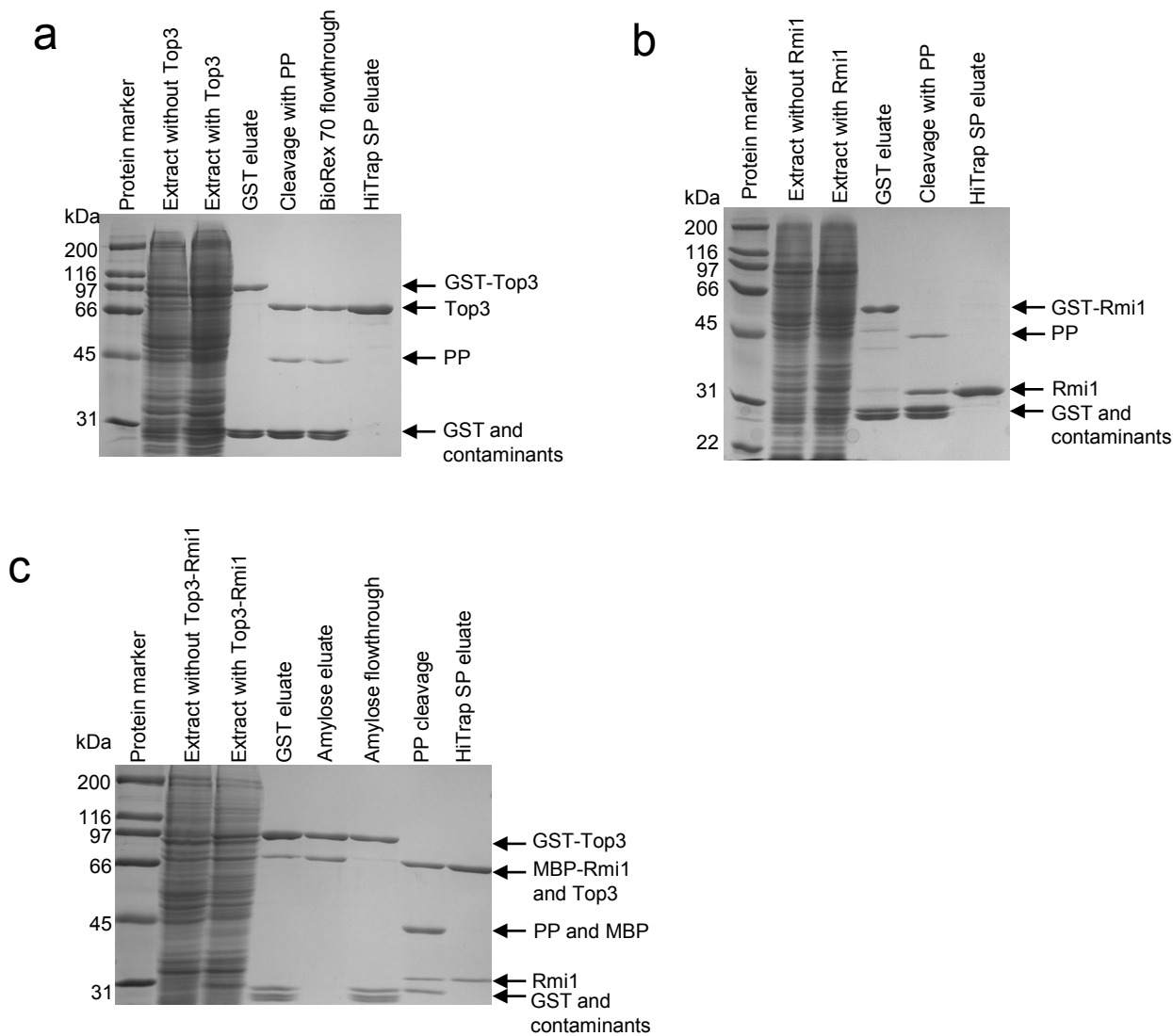
Supplementary Figure 8 Purification of Top3, Rmi1, and the Top3-Rmi1 heterodimer proteins. (**a**) Analysis of a representative Top3 purification by SDS-polyacrylamide gel (10%) electrophoresis. During purification, the N-terminal glutathione-S-transferase (GST) tag was cleaved by PreScission protease (PP). (**b**) Analysis of a representative Rmi1 purification by SDS-polyacrylamide gel (10%) electrophoresis. During purification, the N-terminal GST tag was cleaved by PreScission protease (PP). (**c**) Analysis of a representative Top3-Rmi1 heterodimer purification by SDS-polyacrylamide gel (10%) electrophoresis. During purification, the N-terminal GST tag on Top3 protein and the N-terminal maltose binding tag (MBP) on Rmi1 protein were cleaved by PreScission protease (PP). The gels in all panels were photographed after staining with Coomassie Brilliant Blue.